LOW FREQUENCY ACOUSTIC TEST CELL FOR THE EVALUATION OF CIRCUMAURAL HEADSETS AND HEARING PROTECTION

David A. Cartes*, Laura R. Ray, and Robert D. Collier****

* - Department of Mechanical Engineering, Florida A&M University-Florida State University (FAMU-FSU) College of Engineering, Tallahassee, FL 32306, USA

** - Thayer School of Engineering, Dartmouth College, Hanover, NH 03755, USA.

ABSTRACT

Active noise reduction (ANR) technology, based on feedback signal processing, is being applied in commercial communication headsets and provides noise reductions up to 10-20 dB between 50 Hz and 400 Hz. There are, however, many acoustical designs and computational difficulties associated with feedback designs which limit their performance. Current research in feedforward design offers the opportunity for significant improvement in ANR performance. To support this current research in ANR feedforward algorithm development and evaluation, a low frequency acoustic test cell (LFATC) has been designed to provide a uniform and precisely controlled low frequency acoustic measurement environment. The LFATC design is based on the original work of E.A.G. Shaw and G.J. Theisson at the National Research Council of Canada [1] and a prototype LFATC developed by J.G. Ryan, E.A.G. Shaw, A. J. Brammer, and T.G. Zang [2]. The design analysis of the LFATC is based both on a lumped parameter model and a one-dimensional standing wave model. The acoustic performance of this test cell, including a simple floor vibration isolation system, is evaluated experimentally over a wide range of sound pressure levels. A representative set of measurements with a prototype ANR headset illustrates the application of the LFATC.

SOMMAIRE

La technique de réduction active de bruit, basée sur le traitement de signal rétroactif, est appliquée aux écouteurs de communication commerciaux et rend possible des réductions de bruit jusqu'à 10-20 dB entre 50 Hz et 400 Hz. Il ya cependant bien des obstacles de performance acoustique et de calculs à surmonter avec les systèmes rétroactifs. La recherche actuelle sur les modèles "feedforward" promet une augmentation significative de la performance des systèmes de réduction active de bruit. Pour aider cette recherche vers le développement et l'évaluation d'un algorithme "feedforward", une cellule de test acoustique à basse fréquence (LFATC) a été construite pour fournir un environnement de mesure acoustique uniforme et contrôllé avec précision. L'idée de cette cellule est basée sur le travail original de E.A.G. Shaw et G.J. Theisson au Conseil National de Recherches Canada [1] et sur un prototype de LFATC créé par J.G. Ryan, E.A.G. Shaw, A.J. Brammer et T.G. Zang [2]. L'analyse de fonctionnement de notre cellule est basée sur un modèle de paramètres groupés et un modèle d'onde unidimensionnelle stationnaire. La performance acoustique de cette cellule, comprenant un sytème simple de plancher pour isolation vibrationnelle, est evaluée expérimentalement à travers un intervalle large de niveaux de pression sonore. Un groupe représentatif des mesures avec une paire prototype d'écouteurs à réduction active de bruit illustre l'application de notre cellule.

1. INTRODUCTION

The exposure of the human auditory system to high levels of low frequency noise constitutes a serious problem in modern society. The objectives of this paper are to: (1) describe a specially designed low cost, compact laboratory measurement facility for the evaluation of low frequency Active Noise Reduction (ANR) hearing protection systems; and (2) demonstrate the accuracy of the acoustical measurement system for a range of experimental conditions. Passive noise reduction afforded by communication headsets and hearing protectors is a function of the frequency of the environmental noise and is limited in the low frequency range. Figure 1 shows representative passive noise attenuation measurements for hearing protectors compiled from flat plate testing and low frequency acoustic test cell (LFATC) measurements. Passive noise attenuation typically reaches 30 dB above 1kHz but decreases to less than 10 dB below 100Hz. These relatively small reductions are inadequate for hearing protection in high noise level environments dominated by low frequency noise. The adverse effects of high intensity low frequency sound, including the effect of the upward spread in masking at higher frequencies, are summarized in reference [3].

Active Noise Reduction (ANR), based on feedback designs, has been developed and implemented in commercially available headsets over the past decade. Figure 2 illustrates representative objective measurements reported for current technology ANR feedback headsets compiled from LFATC testing and MIRE testing. Included in Figure 2 are upper and lower noise reduction performance bands for feedback headsets from [4]. Reductions of the order of 10-20 dB over a frequency range of 50-400 Hz are measured for stationary broadband white noise introduced through multiple speaker systems in reverberant rooms. It is well known that the performance of feedback ANR headsets is highly dependent on the specific characteristics of the incident noise and that the feedback circuitry and signal processing often adds to the noise in the mid-frequency speech communication bands [5]. Due to the limitations of feedback ANR headsets, recent research has focused on development of feedforward ANR based on least-mean-squared (LMS) adaptive filters [6-11]. The schematic of a feedforward ANR system is shown in Figure 3, and Figure 2 provides sample active noise reduction measurements of feedforward ANR in response to pure tones, from [6].

The variable spatial and temporal acoustic environments of reverberant testing room facilities are inadequate to support the precision measurements required for research and development investigations in advanced feedforward ANR algorithms and prototype headset designs. The need is to establish a highly controlled noise field in which the performance and stability of specific ANR algorithms, in conjunction with actual headset hardware configurations, can be accurately measured and compared. The source noise fields must include a wide range of conditions from deterministic

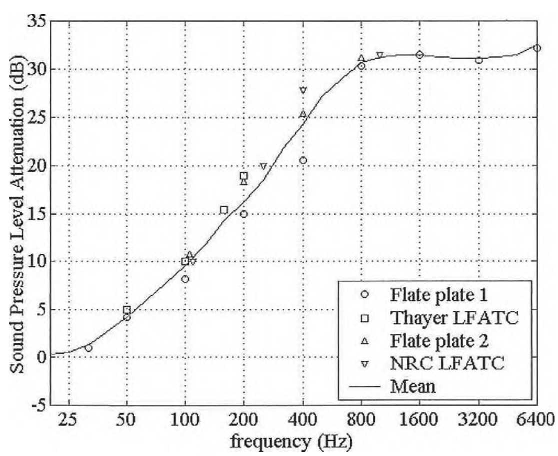

Figure 1. Representative passive noise attenuation in flat plate testing and LFATC testing of hearing protectors.

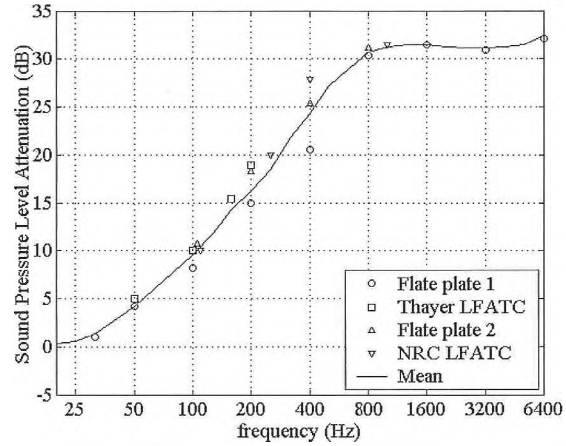

Figure 2. Representative active noise reduction in MIRE and LFATC testing of feedback and feedforward headsets.

discrete frequency tones to broadband non-stationary and narrowband impulsive sources.

The development of a low frequency acoustic test cell (LFATC) has been an important component in the feedforward ANR research of Dr. Anthony Brammer and his colleagues at The National Research Council (NRC), Ottawa, Canada. Their prototype LFATC design was based on the original work of Shaw and Theisson [1] and is described in reference [2]. Results of the research are reported in references [6-9].

In 1998, the authors initiated research in feedforward LMS algorithms for low frequency noise reduction in communication headsets as part of a Unites States Air Force sponsored program. A major goal of the Thayer research has been to develop and evaluate the performance and stability of innovative adaptive leaky LMS algorithms based on Lyapunov tuning principles [10]. As was the case for the NRC program, this research requires precise acoustic measurements under rigorously controlled experimental conditions involving high intensity noise levels up to 140 dB, a wide dynamic range, and real world, highly non-stationary jet aircraft noise. The design and construction of the Thayer LFATC are presented in this paper together with examples of the measurements obtained with this facility. A comprehensive description of the experimental results of this research program is given in reference [11].

The modified LFATC specifically addresses the need for vibration isolation, providing a sufficiently low noise floor to demonstrate feedforward ANR over a wide dynamic range. Moreover, the design extends the cut off frequency of the LFATC up to 200 Hz, as compared to 100 Hz in the NRC prototype LFATC reported in [2]. Additional design and fabrication refinements provide a functional laboratory measurement system for testing communication headsets.

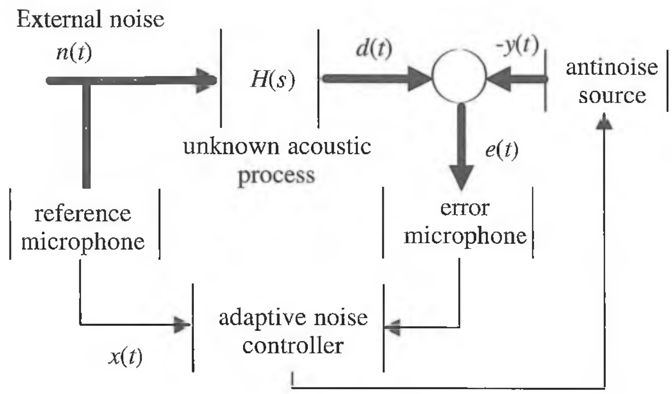

Figure 3. Single channel feedforward active noise control. Thick lines represent acoustic signals, thin lines represent electrical signals.

2. LFATC DESIGN

The specifications for the Thayer LFATC are as follows:

Frequency range:	20-200 Hz; uniform response
Dynamic range:	65 dB; Source levels, 75-140 dB
Noise floor:	50 dB in headset
Wall thickness:	Min. 50 dB transmission loss
Signal-to-noise ratio for experiments:	30 -50 dB in headset
Loudspeaker:	High fidelity with minimum distortion at up to 140 dB

These specifications are predicated on three principle performance requirements: (1) precise, direct sound pressure measurements over the frequency band for maximizing ANR performance without filters or equalizers; (2) evaluation of ANR algorithms over a 65 dB range of noise levels within the headset; and (3) operation in normal laboratory quiet environments.

Two models were employed in the LFATC design, namely a lumped parameter model and a one-dimensional standing wave model. Use of the two models is dictated by the predicted dimensions, i.e., lumped parameter, one-dimensional and multi-dimensional models are based on the ratio of wavelength, , to a major dimension [12]. The measured broadband response is represented by both the lumped parameter and the standing wave model. First, a given topology is assumed which establishes the physical relationships of the proposed system as shown in Figure 4.

The cylindrical test cell wall is made of aluminum (6061-TS), which provides both the required stiffness for the rigid wall assumption and the mass for the required high transmission loss. The inner wall is lined with a sound absorbing felt wool material to minimize higher frequency cross modes. This lining, which is made of 95% natural wool

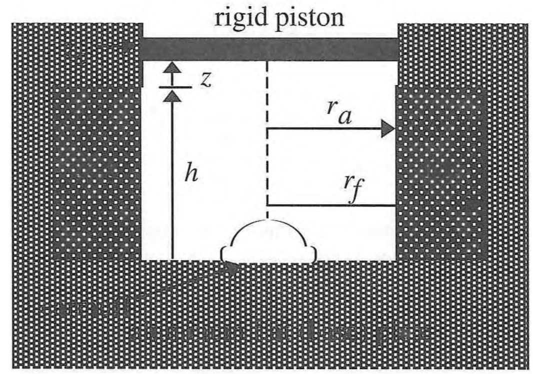

Figure 4. Low frequency acoustic test cell topology showing critical dimensions and placement of earmuff.

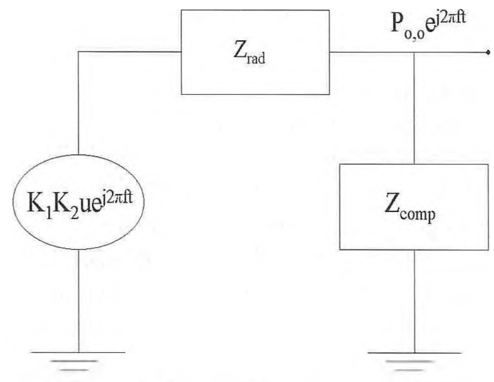

Figure 5. Lumped parameter model.

and has a density of 342 kg/m^3 and a thickness of 3.81 cm, is not included in the models. The acoustic medium is air at T= 30 C and humidity of 70%.

The critical dimensions for the topology are shown in Figure 4. The test cell is a right cylinder with critical dimensions of height of test volume, h, radius of air column, r_a, and radius of felt annulus, r_f. The test cell's excitation is provided by a speaker which is modeled as a rigid piston of radius r_a, at a height z. z_o is the mean position of the piston's radiating surface. The objective of this model is to determine the pressure, $P_{0,0}\, e^{2\pi ft}$, at the center of the base plate surface contacting the air column, $(h,\ r_a)$ = (0 cm, 0 cm), on which a prototype circumaural headset is to be mounted.

Figure 5 gives the equivalent lumped parameter model for the LFATC, where f is the frequency, $Ue^{2\pi ft}$ is the volume velocity (m/s), and K_1 is the constant speaker gain (N-sec/volt-m^2). Z_{rad} (N-s/m^5) is the radiation impedance into the LFATC and Z_{comp} is the compliance impedance associated with the test volume. The following equations are given in Beranek [12] for $kr_a < 0.5$, where k is the wave number:

$$Z_{rad} = 6\frac{\rho r_a^2 \pi^4 f^4}{c^3} \tag{1}$$

$$Z_{comp} = \frac{-j\pi(r_f^2 h + r_a^2 z_0)}{\rho c^2 2\pi f} \tag{2}$$

The estimated values for density, ρ, and speed of sound in air, c, provide a closer forecast of subsequent LFATC experimental calibration. Conversely, use of the LFATC is not limited to these experimental conditions.

Given the impedance expressions in eq. 1 and 2, the transfer function, $H(f)$, of the lumped parameter model is

$$H(f) = \frac{K_1 Z_{comp}}{Z_{comp} + Z_{rad}} \tag{3}$$

For standing wave pressures, the internal volume of the test cell is modeled as a one-dimensional wave-guide. This is an acceptable approximation as long as the shell diameter, $2r_f$, is less than one-tenth the wavelength, 0.1λ. The problem is to find a single ray's interaction with the test cell's termination flange and speaker diaphragm as it reflects between the source and the base flange, and then to integrate to capture all excitation generated by the source at steady state. The point source, P_s is modeled as

$$P_s(f) = K_2 K_1 U e^{j2\pi ft} \tag{4}$$

where K_2 is a unitless correction factor, which is necessitated by the fact that ambient values of the lumped-parameter and standing wave models must agree. Air has a linear attenuation factor, δ, that describes the attenuation of sound per unit length of a ray's travel. At each surface reflection, the surface pressure is the sum of the incident wave and the reflected wave. The reflected wave is reduced by the reflection coefficient, α, for the flange and β, for the diaphragm. The calculation of reflection coefficient for aluminum is

$$\alpha = \frac{Z_{aluminum} - Z_{air}}{Z_{aluminum} + Z_{air}} \tag{5}$$

As the ray passes between surfaces it is also phase shifted with respect to the source due to the distance traveled by a factor, $-kx$. x the distance between the diaphragm and terminal flange. The resultant infinite series is

$$P_f(t,f,x) = K_1 K_2 U \sum_{i=1}^{\infty} \delta^{2i-1}(\alpha^{i-1} + \alpha^i)\beta^{i-1} e^{j(2\pi ft-(2i-1)kx)} \tag{6}$$

whose magnitude for this instance can be simplified as an infinite geometric series to

$$P_f(f) = K_1 K_2 U \frac{(1+\alpha)\delta e^{-j2\pi f(h+z_o)/c}}{1-\delta^2 \alpha\beta e^{-j4\pi f(h+z_o)/c}} \tag{7}$$

The net magnitude of the sound pressure level for the LFATC is expected to be some weighted combination of the two models. For example,

$$P = 20\log_{10}\left[\frac{\left(w_1|H(f)| + w_2|P_f(f)|\right)}{20\mu Pa}\right] \text{dB} \tag{8}$$

where w_1 and w_2 are weighting factors. This model is valid for frequencies below $\lambda/10$ or

$$f = \frac{c}{20 r_f}. \tag{9}$$

The first resonant frequency, f_r, for this model is

$$f_r = \frac{c}{2(h+z_o)}. \tag{10}$$

The design parameter values given in Table 1 were chosen to provide minimum clearance between the headset earmuff under test, and the noise source speaker. Figure 6 shows the predicted results of eq. 8 with weighting factors w_1=w_2=0.5, which are compared with the actual experimental data as discussed in Section 4. Using the test cell dimensions of Table 1, a uniform low frequency plane wave pressure field is predicted for 0-200 Hz. The magnitude of the sound pressure field is predicted to decrease by about 6 dB in the 200-400 octave band. The first resonance, predicted by eq. 10, is at 1580 Hz, which is well beyond the measurement range of the cell.

3. LFATC DESCRIPTION AND ISOLATION

Based on model simulations, the LFATC, shown in Figures 7 and 8, is constructed following the pattern in Ryan et al. [2]. The LFATC is constructed from 1.27 cm thick aluminum (6061 – T5) plate and cylinder. It rests on an aluminum flat plate base of dimensions 43.18 x 43.18 x 10.16 cm. The upper chamber is assembled from a cylinder 12.7 cm long with an inside diameter of 22.86 cm. It is terminated with a 7.62-cm thick aluminum plug. The remaining 5.08 cm depth of the upper chamber is filled with felt, except for that portion occupied by the back of the speaker. The lower chamber's dimensions are given in Table 1 and its wall is covered by a 3.81-cm thick annulus of felt. The horizontal gasket, labeled damping in Ryan et al. [2], is omitted. A 15.24-cm diameter Rockford Fosgate 100-watt speaker,

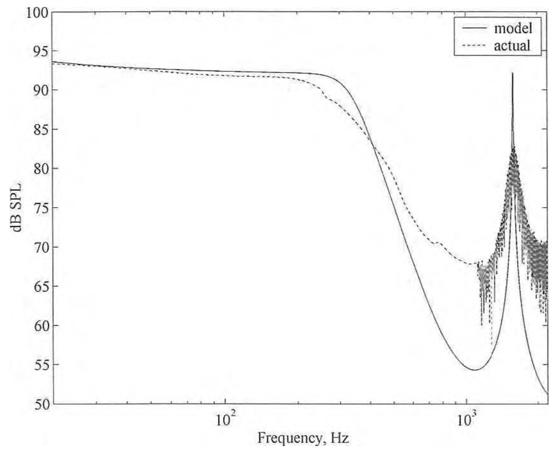

Figure 6. Comparison of model and experimental frequency response.

model FNQ1406, provides the sound source. A B&K (4190) precision microphone is mounted axially in the center of the base. Another precision microphone is mounted radially through the midpoint of the lower volume cylinder wall. This dual microphone arrangement allows the simultaneous measurement of acoustic pressures both internal and external to the communication headset.

A flat plate headset attachment is provided by two 0.32-cm eyebolts, mounted 5.08 cm radially from the axis to which precision dental ligatures are attached. The end of each ligature is attached to studs protruding from the headset. This arrangement ensures a uniform seal pressure between the headset cuff and the flat plate.

Extensive rotating machinery in adjacent spaces and construction at a nearby facility necessitated the isolation of the LFATC from the floor of the laboratory. Accordingly, the LFATC is isolated from the floor by using two layers of air packing material, 30.48 cm in diameter, separated by a 50.8 x 63.5 x 1.27-cm brass plate. The test cell is supported on this isolation by a 50.8 x 63.5 x 1.27-cm plywood bed. The compressed height of the plywood bed from the floor is 45.72 cm.

4. LFATC CALIBRATION DATA

Figure 9 shows the noise floor within the test cell volume as measured at the base of the test cell, $(h, r_a) = (0 \text{ cm}, 0 \text{ cm})$, by the installed B&K microphone. This noise floor establishes the maximum performance level of active noise reduction measurable in the test cell. The 'without' vibration isolation indicates the noise floor obtained with the LFATC sitting directly on the lab floor. The vibration isolation provides a 45 dB reduction in the noise floor in the 50-60 Hz range and a lower threshold of 50 dB for the sound pressure level is satisfied above 50 Hz. At 20 Hz the noise floor limits the lowest sound pressure level to 60 dB. A test consisting of discrete pure tones was performed throughout the band of interest at the maximum design pressure level of 140 dB to verify the performance of the test cell. No difference was found in the noise floor as measured at the B&K microphone within a mounted headset and without a headset in place.

The predicted frequency response and characteristics of the gradient pressure field within the LFATC were verified

Table 1. Design parameters.

Parameter	Value
ρ_{air}	1.293 kg/m^3
c_{air}	334 m/s^2
r_a	7.62 cm
r_f	3.81 cm
h	7.62 cm
z_0	2.96 cm
$Z_{aluminum}$	1.7 x 10^7 Ns/m^5
$Z_{speaker}$	0.9 x 10^7 Ns/m^5
δ	0.996 m^{-1}

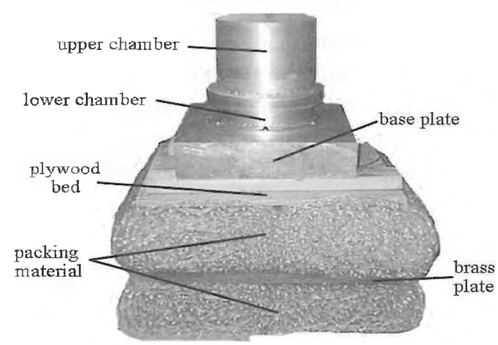

Figure 7. Assembled view of the LFATC.

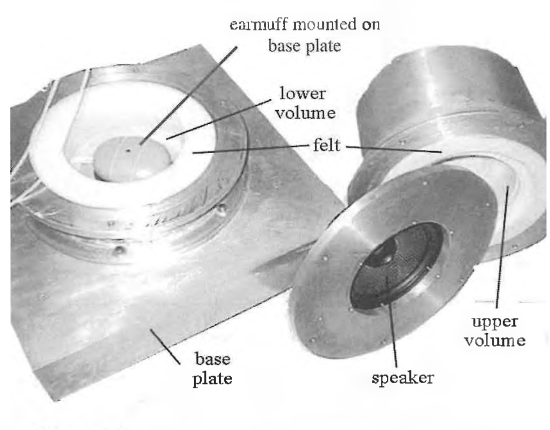

Figure 8. Disassembled view of theLFATC.

experimentally. The speaker was chosen to have sufficient power rating and dynamic range to make the transfer function magnitude a constant gain, K_I, in the frequency band of interest. The excitation for the experiment was a 2-volt peak-to-peak chirp from 1 to 10 KHz of 2 minutes duration. The results are shown in Figures 6, along with the theoretical frequency response predicted by eq. 8.

The transfer functions based on experimental data for three positions on the LFATC axis, (h, r_f) = (0 cm, 0 cm), (2.54 cm, 0 cm), and (5.08 cm, 0 cm), are shown in Figure 10. Experimentally, the quality factor, Q, is significantly lower than predicted due to the felt liner in the actual LFATC. A second experiment using a 0.2-volt peak-to-peak excitation, an order of magnitude lower than the previous experiment, was conducted to show linearity. These transfer functions, which are not shown, show no perceptible differences from those in Figure 10.

These results demonstrate a linear test volume exists between 20 and 200 Hz and 50 and 140 dB. Indeed, the results of this calibration, as seen in Figures 6 and 10, indicate that the LFATC has the properties to permit measurements up to 1000 Hz, or two or more octaves above the 50-200 Hz frequency range chosen for the experimental evaluation of ANR algorithms.

5. LFATC Practical Demonstration

As previously mentioned, the authors are performing research in low frequency, feedforward ANR algorithm development and evaluation for communication headsets. This research requires experimental comparison of candidate ANR algorithms that are variants of the LMS family of algorithms. Candidate algorithms have been developed based on a Lyapunov tuning method described by the authors in [10]. These algorithms are variants of the well-known leaky, normalized LMS (LNLMS) algorithm [13] and are designed to optimize both low frequency stability and active noise reduction performance over a large dynamic range for non-stationery noise sources. The Lyapunov tuned algorithms provide a time-varying leakage factor and step-size combination that retains acceptable stability of the weight update equation at low signal-to-noise ratio (SNR) on the measured reference input, while maximizing ANR performance at both low and high SNR. The Lyapunov tuning method also addresses the need to eliminate empirical tuning of LNLMS algorithms. The use of the LFATC is demonstrated by comparison of a Lyapunov-tuned algorithm to traditional normalized (NLMS) and fixed-leakage factor LNLMS algorithms in conjunction with a prototype headset, with highly non-stationary, F-16 aircraft cockpit noise. The F-16 noise is band limited to 50 Hz due to the high distortion levels of the small, commercially available, noise cancellation headset speakers operating at high reference sound pressure levels.

Low and high SNR performance comparisons of a Lyapunov-tuned leaky, normalized LMS algorithm to a fixed leakage factor LNLMS and NLMS algorithms are shown in Figures 11 and 12, respectively. Noise reduction performance is measured at the prototype headset's error microphone. The figures represent the ensemble average of four sets of independent measurements. In Figure 11, at low SNR the NLMS algorithm is unstable, due to weight drift induced by measurement noise on the reference input. Instability is indicated by a non-convergent sound pressure level (SPL) within the five-second sample. The constant leakage factor LNLMS filter is empirically tuned to regain stability at low SNR, resulting in a performance degradation of approximately 10 dB. The Lyapunov-tuned LMS filter is shown to provide stability, while enhancing noise reduction performance over the fixed-leaky LNLMS filter by 5 dB.

When these algorithms are applied at high SNR, as

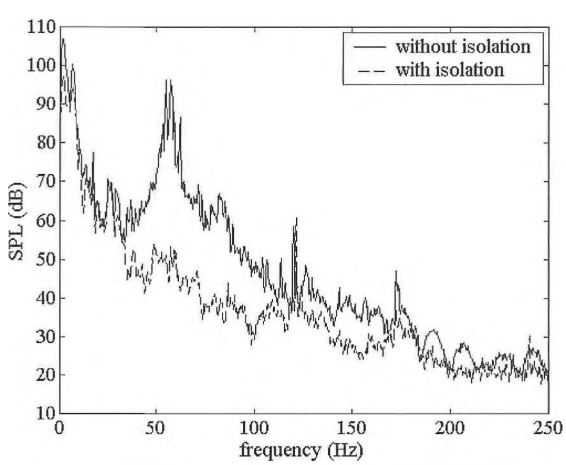

Figure 9. Noise floor measured at bottom center of the base plate at the B&K without and with vibration isolation.

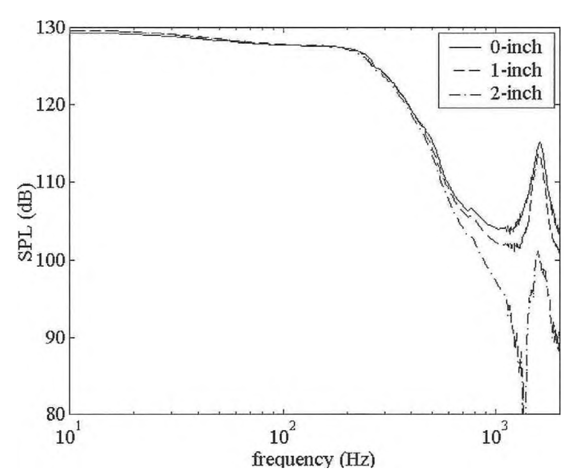

Figure 10. Linearity test at 3 locations from the bottom center of the base plate.

shown in Figure 12, the NLMS filter remains unstable, though the divergent behavior is imperceptible in the five-second sample. Nevertheless, the NLMS filter performance provides the "best case" target noise reduction performance for the family of normalized LMS algorithms. Again, the fixed-leaky LNLMS filter results in a performance degradation of 10 dB. The Lyapunov-tuned LMS filter is stable and provides no ANR performance degradation over the NLMS filter.

These results demonstrate that the Lyapunov-tuned filter has performance characteristics approaching the NLMS filter at high SNR, while retaining stability at minimal performance degradation at low SNR, compared to an empirically tuned fixed leakage factor LNLMS filter. In Figure 11, the minimum SPL attained is well above the 50 dB noise floor design specifications. The LFATC provides a precise

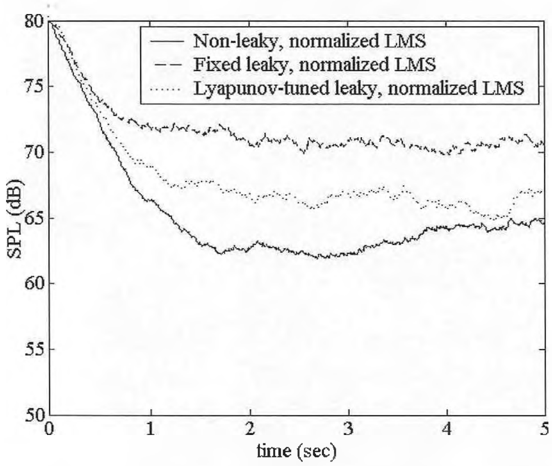

Figure 11. Comparison of three LMS algorithms canceling 80 dB F-16 noise inside the prototype headset. This represents the performance potential during low SNR, 35 dB.

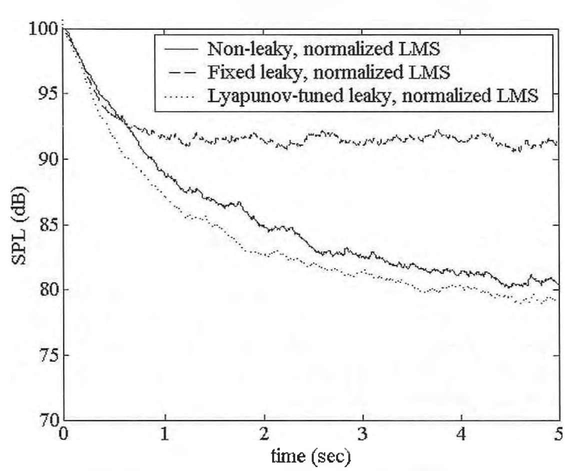

Figure 12. Comparison of three LMS algorithms canceling 100 dB F-16 noise inside the prototype headset. This represents the performance potential during high SNR, 55 dB.

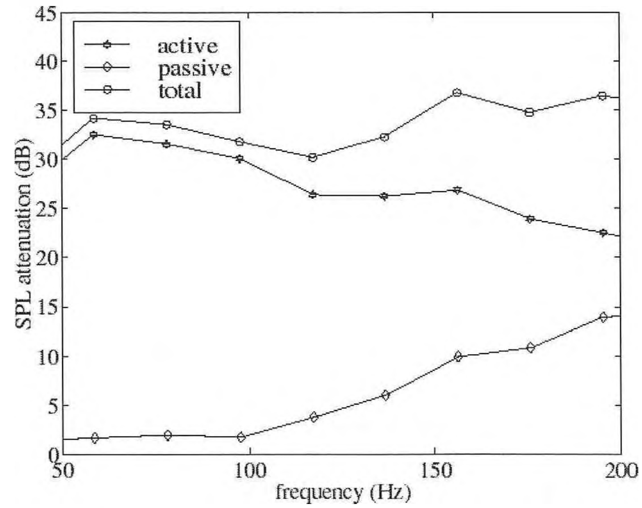

Figure 13. Prototype headset noise reduction performance at the error microphone.

evaluation of convergent, divergent, and steady state performance of prototype headsets and ANR algorithms as a function of SNR.

Figure 13 shows the passive attenuation, active noise reduction, and combined noise reduction performance of the Lyapunov-tuned leaky NLMS algorithm at the error microphone of the prototype headset in response to a sum of pure tones, {50, 63, 80, 100, 125, 160, 200} Hz. The passive attenuation values of the prototype headset were somewhat lower than those values shown in Figure 1 for commercial headsets due to wiring modifications. On the other hand, compared to the best-case active performance of feedback ANR headsets presented in Figure 2, measured active noise reduction using the Lyapunov tuned algorithm provides an additional 10-20 dB active noise reduction in the 50-200 Hz frequency band.

6. CONCLUSIONS

A linear acoustic test volume for the evaluation of low frequency active noise reduction in circumaural headsets and hearing protection has been designed, constructed, and validated experimentally. The LFATC volume dimensions are derived using two acoustic models in its design. These are a lumped-parameter model and a one-dimensional standing wave model. The vibration isolation system provides up to a 45 dB improvement in the noise floor within the bandwidth of interest. This LFATC has been used to evaluate feedforward ANR algorithms and communication headsets in the bandwidth of 50-200 Hz over a dynamic range of 65 dB.

ACKNOWLEDGEMENT

The authors are grateful to Dr. Anthony Brammer for his insight and suggestions in the development of the LFATC. This research is sponsored by the United States Air Force through contract number F41624-99-C-6006, under a sub-contract with Creare, Inc.

REFERENCES

[1] E.A.G. Shaw and G.J. Theissen, " Improved Cushion for Ear Defenders", J. Acoust. Soc. Am., vol 30, 1958.

[2] J.G. Ryan, E.A.G. Shaw, A.J. Brammer, and G. Zang, "Enclosure for Low-Frequency Assessment of Active Noise Reducing Circumaural Headsets and Hearing Protectors," Canadian Acoustics, pp. 19-20, 1993.

[3] W. Dixon Ward, "Effects of High Intensity Sound", Chapt.119, Encyclopedia of Acoustics, edited by Malcolm J. Crocker, John Wiley & Sons, Inc. 1997.

[4] A. Akelsson, ed. "Scientific Basis of Noise-Induced Hearing Loss," Proceedings of the 5th International Symposium on the Effects of noise on Hearing, May 1994: Thiem Medical Publishers, Inc., 1996.

[5] R.L. McKinley and C.W. Nixon," Active Noise Reduction Headsets", Proc. 6th International Conference on Noise as a Public Health Hazard, Nice, vol.2, pp 83-86. 1993.

[6] G.J. Pan, A.J. Brammer, and R.B. Crabtree, "Adaptive Feedforward Active Noise Reduction Headset for Low-Frequency Noise," Proc. Symposium on Active Control of Sound and Vibration, Edited by Elliott and Horvath, 1997.

[7] R.B. Crabtree, " Real-World Performance of Headset Active Noise Reduction Systems," 136th Meeting, Acoustical Society of America, October 1998.

[8] G.J. Pan, A.J. Brammer, R. Goubran, J.G. Ryan, and J. Zera, "Broad-Band Active Noise Reduction in Communication Headsets," Canadian Acoustics, 22(3), pp. 113-114, March 1994.

[9] A.J. Brammer and G.J. Pan, "Opportunities for Active Noise Control in Communication Headsets," Canadian Acoustics 26(3), pp. 32-33, September 1998.

[10] D. Cartes, L.R. Ray, and R.D. Collier, "Lyapunov Tuning of the Leaky LMS Algorithm for Single-Source, Single-Point Noise Cancellation." Proceedings of the American Control Conference, pp. 3600-3605, 2001.

[11] D. Cartes 2000 Lyapunov Tuning and Optimization of Feedforward Noise Reduction for Single-Point, Single-Source Cancellation, Ph.D. dissertation, Thayer School of Engineering, Dartmouth College, October 2000.

[12] L.L. Beranek, Acoustics, American Institute of Physics, 1986.

[13] S.M. Kuo and D.R. Morgan, Active Noise Control Systems: Algorithms and DSP Implementations, John Wiley& Sons, Inc., 1996.